TSINGHUA SCIENCE AND TECHNOLOGY
ISSN 1007-0214 02/16 pp377-384
Volume 15, Number 4, August 2010

Synthesis and Characterization of Ordered Meso-Macro-Porous Silica Membranes on a Porous Alumina Support*

Duo Li, Y.S. Lin**, V.V. Guliants†

Department of Chemical Engineering, Arizona State University, AZ 85287, USA;
† Department of Chemical and Materials Engineering, University of Cincinnati, OH 45221, USA

Abstract: Macroporous silica materials with ordered three-dimensional pore structure can be easily prepared by the template-directed sol-gel process. However, it is still a challenge to prepare them in membrane form on a porous support, which limits their applications. In this work, we have demonstrated the feasibility of obtaining a three-dimensional ordered macroporous silica membrane on macroporous alumina support using poly-methyl methacrylate (PMMA) spheres as the template. PMMA spheres were packed on the top of an Anopore-alumina support by filtration of a PMMA aqueous suspension. Silica sol obtained by an acid-catalyzed sol-gel process was infiltrated into the voids among the spheres. Drying induced stress caused the membrane to crack or peel off from the top of the support. This can be minimized by annealing the PMMA template layer before the introduction of silica sol which increases the mechanical strength of the template. Calcination or solvent extraction to remove the template produced a highly ordered three-dimensional macroporous silica membrane with spherical pores connected by windows in the mesoporous range. The results show that the PMMA-templated infiltration method is effective in preparing three-dimensional ordered macroporous silica membranes on a porous support.

Key words: macroporous; ordered; silica; membrane

Introduction

Ordered three-dimensional (3-D) macroporous silica materials including synthetic opal and reverse opal silica have many applications in catalysis[1], photonic technology[2], drug delivery[3], and chemical sensors[4] due to their well-defined structure, precisely controlled pore size and surfaces that can be chemically functionalized. Recent studies also showed that the ordered macroporous silica may be employed in chemical separation. Cichelli and Zharov[5] reported the separation of chiral molecules using synthetic opal modified with a chiral selector moiety and the selectivity observed was comparable to antibody-modified nanotube membranes. Zeng and Harrison[6] reported the size-based separation of biomolecules ranging from proteins smaller than 10 nm to long DNA coils of about micrometer size using synthetic opal structures. Zheng et al.[7] reported high-speed electrochromatographic separation of cationic dyes and peptides based on differences in adsorptivity and electrophoretic mobility using synthetic opal.

The synthetic opal structure has a porosity of about 26% and can be prepared by self-assembly of colloidal silica spheres. In comparison, the reverse opal materials have a porosity of about 74%, which results in much faster mass transfer rate, and therefore, are preferred for many applications involving mass transfer. Reverse opal materials can be prepared by the latex spheres templating method, which typically consists of three steps[8]. First, monodisperse latex spheres are self-assembled into ordered 3-D arrays (the same

Received: 2010-05-28
* Supported by the National Science Foundation (No. CTBE-0403897)
** To whom correspondence should be addressed.
E-mail: Jerry.Lin@asu.edu

structure as in the case of synthetic opal) either by gravity sedimentation[9], crystallization via repulsive electrostatic interactions[10], or self-assembly under physical confinement[11]. In the second step, the interstitial voids of the ordered 3-D arrays are filled with precursors of ceramics, metals, or polymers. The precursors are then hydrolyzed and condensed to form a solid framework in the voids among the spheres. Finally, removal of the template either by calcination or solvent extraction produces highly ordered 3-D reverse opal materials with interconnected spherical pores.

For applications involving mass transfer, such as chemical separation, the reversed opal material should be prepared in the form of a membrane, i.e., as a thin film on a porous support. However, most existing techniques for the fabrication of the ordered 3-D array templates can only produce either free standing colloidal arrays or arrays on dense substrates, such as free standing polystyrene template using centrifugation[12], silica spheres templates on quartz microscope slides by using solvent evaporation[13], and polystyrene template on silicon wafers using vertical convective self-assembly[14]. It is difficult to prepare reverse opal silica in a membrane geometry on a porous support, because the self-assembly of the colloidal template on a porous support not only depends on the suspension concentration, but also on the pore size, pore morphology, and the surface roughness of the substrate. Also, the thin film on the support could easily crack due to the stress induced by the high percentage (more than 20%) of volume shrinkage of the inorganic framework during the drying of the silica sol and the following template removal process[14].

In this paper, we report the synthesis of ordered macroporous reverse opal silica thin films on porous support by a new filtration method. Polymethyl methacrylate (PMMA) spheres were packed on an Anopore alumina support by filtration, followed by annealing to enhance the mechanical strength of the template layer. Multiple infiltrations of silica sol were conducted to fill the cracks generated during drying. The template was removed by solvent extraction to minimize the shrinkage during template removal. The prepared silica materials had interconnected spherical pores with windows about 1/7 of the diameter of the template spheres and are highly promising for applications in chemical separation.

1 Experimental

1.1 Membrane preparation

PMMA spheres with a ~240 nm diameter were prepared by the surfactant-free emulsion polymerization method. First, argon was bubbled for at least 20 min through 175 g of deionized (DI) water in a high density polyethylene bottle to remove dissolved air. Then, 20 g of methyl methacrylate (Acros) was added to the degassed DI water. The mixture was kept at 70℃ in a water bath under constant stirring for at least 15 min. 5 g of 2 wt.% of 2, 2'-Azobis [2-(2-imidazolin-2-yl) propane] dihydrochloride (coded V_{A-44}, WAKO Chemical, Japan) was injected as an initiator into the methyl methacrylate solution mentioned above. After 8 h, the reaction was stopped by cooling the solution down to room temperature.

PMMA spheres were packed on an Anopore alumina support (Whatman, USA) with pore size 200 nm in order to prepare macroporous silica membranes by the filtration method. A stirred cell (Millipore) was used as the filtration apparatus. Vacuum was applied on the downstream side of the cell. After a few hours, PMMA spheres were self-assembled into ordered 3-D arrays on the top of the support. The vacuum filtration was stopped, and the supported 3-D PMMA arrays were dried in a humidity-controlled climate chamber in air at 40℃, 40% relative humidity, and atmospheric pressure overnight, and then moved to an oven and annealed at 130℃ for 1 h. This template was used to prepare the macroporous silica membrane on Anopore support.

Silica sol was prepared by nitric acid-catalyzed hydrolysis and condensation of tetraethyl orthosilicate (TEOS) (Aldrich)[15]. The molar ratio of the ingredients was TEOS: ethanol: nitric acid: DI water = 1: 3.8: 0.09: 6.5. Mixtures of TEOS/ethanol and nitric acid/water were prepared separately. A 3-neck round flask was preheated to 60℃, and then the mixtures were slowly added into the flask. A condenser was connected to reflux the reactant vapors. The mixture in the flask was stirred for 3 h at 60℃ and then cooled down naturally to room temperature.

The prepared silica sol was then dropped on the template layer. The voids in the PMMA template layer

on the Anopore support were then infiltrated with the silica sol by the capillary force. Vacuum was applied to remove the excess silica sol to prevent the formation of a dense silica layer on the top of 3-D arrays. The vacuum filtration was stopped when the template layer was uncovered. After drying at 80℃ for 10 min, a microstructured SiO_2 network formed in the voids among the spheres shrank. Repeating the infiltration and drying 8 times allowed the silica network to fill the voids completely. The template was removed by either calcination at 550℃ in air for 3 h or one-time solvent extraction with 1:1 (*v*/*v*) mixture of tetrahydrofuran and acetone for 5 d.

1.2 Characterization

The morphology of the membranes was characterized by scanning electron microscopy (SEM) (Phillips XL-30 ESEM scanning microscope). Samples were attached to a metal mount using carbon tape, and then coated with ~8 nm thick gold layer by plasma sputtering to avoid sample charging. The glass transition and decomposition temperatures of the PMMA spheres were analyzed by thermogravimetric analysis and differential scanning calorimetry (TGA-DSC) (TA Instruments SDT Q600). The sample was heated from 50℃ to 550℃ at a ramping rate of 5℃/min in air flow. The light transmittance of samples was measured by UV-visible. Nitrogen adsorption and desorption isotherms of sol-gel silica (prepared without the template) and ordered macroporous silica materials were measured at −196℃ using a Micromeritics ASAP 2020 system. The samples were degassed first at 90℃ for 1 h and then at 200℃ for 5 h. The pore size distribution of micropores was calculated by the H-K method and that of mesopores by the BJH method.

2 Results and Discussion

2.1 PMMA spheres and 3-D arrays

Monodisperse PMMA spheres were produced in large quantity by the emulsion polymerization method. The PMMA suspension contained 10 wt.% of solids. Figures 1a and 1b are the SEM images of the PMMA spheres prepared by emulsion polymerization without and with the surfactant. It may be observed that the PMMA spheres prepared by the surfactant-free method have diameters of ~280 nm, much larger than the PMMA spheres prepared with surfactant (~50 nm diameter). The difference in size is caused by the difference in the surface charge density of PMMA spheres. The larger surface charge density for the PMMA spheres prepared with surfactant due to the adsorption of surfactant molecules on sphere surface prevents the aggregation of the spheres to form larger spheres[16]. By changing the experimental conditions, such as the initiator concentration and polymerization temperature, PMMA spheres with different diameters from 50 nm to about 1 μm can be synthesized.

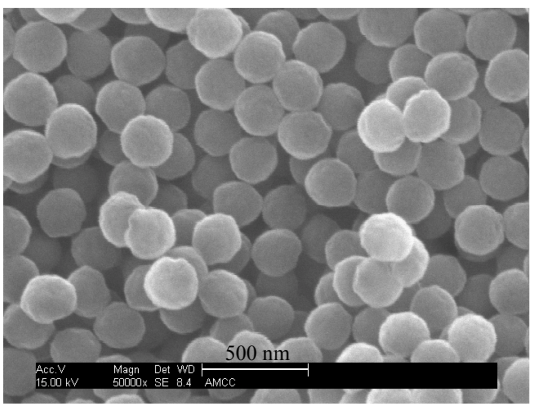

(a)

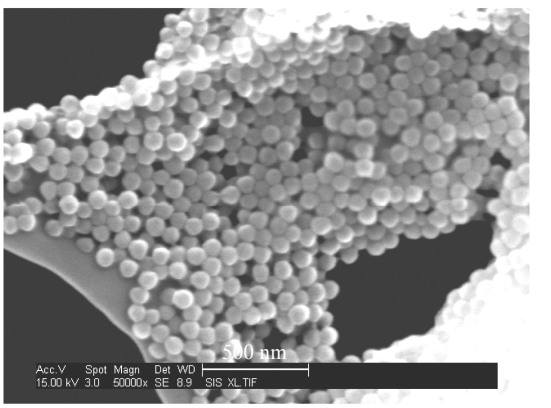

(b)

Fig. 1 SEM images of PMMA spheres prepared by (a) surfactant-free emulsion polymerization method and (b) emulsion polymerization with surfactant

To prepare free-standing macroporous silica, PMMA arrays were obtained by centrifugation at 4000 r/min, followed by drying at 40℃ overnight. The PMMA spheres underwent disorder-order transition from their suspension to the highly organized colloidal crystals through the application of the centrifugal force. Figure 2 shows the SEM images of the PMMA array. Figure 2a shows 2-D hexagonal pattern of PMMA spheres, which is indicative of the (111) plane of the

face-centered-cubic (fcc) lattice or the (001) plane of the hexagonal close-packed (hcp) lattice. The square pattern of the PMMA spheres in Fig. 2b is consistent with the (100) plane of the fcc lattice and inconsistent with hcp lattice, which confirmed that the PMMA array had fcc structure. This observation agrees well with the conclusions of Woodcock, in which they reported that the preference of a fcc structure over the hcp one was due to the Gibbs free energy difference between these two phases of a crystal of hard spheres[17].

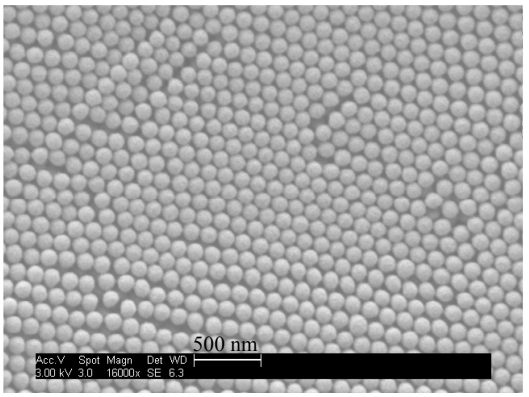

(a) Hexagonal PMMA arrays

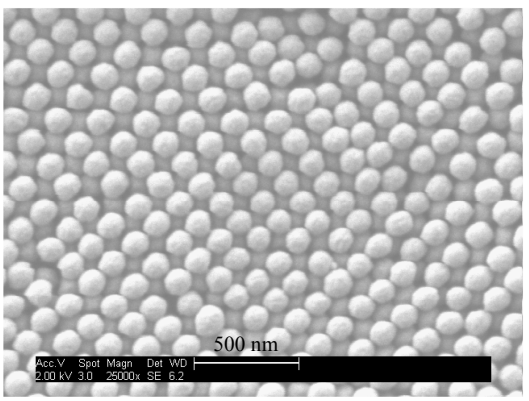

(b) Body-centered-cubic PMMA arrays

Fig. 2 SEM images of the PMMA array

PMMA spheres were packed on an Anopore alumina support by filtration. The thickness of the template layer can be easily controlled within 10 microns by varying the amount and the concentration of the suspension solution being filtered. The 3-D arrays obtained exhibited some color reflections when observed from different angles due to the diffraction of light from the ordered lattices. PMMA arrays on the Anopore support had fcc structure with lattice parameter of $\sqrt{2}\,d$, which is 396 nm (d is the diameter of PMMA spheres). The light transmittance spectrum of the ordered arrays is shown in Fig. 3. The minimum light transmittance at about 565 nm is due to the Bragg's reflection. The propagation of light in the ordered lattices at that wavelength is strongly prohibited, resulting in a dip in the transmission spectrum known as a stop band[18]. The spectral position of the stop band depends on the lattice parameter related to the diameter of the PMMA spheres, and the effective refractive index of the fcc structure according to the modified Bragg law[19]:

$$m\lambda = 2d_{(\mathrm{hkl})}\sqrt{n_{\mathrm{eff}}^2 - \sin^2\theta} \tag{1}$$

where m is an integer, λ is the wavelength of the electromagnetic wave, $d_{(\mathrm{hkl})}$ the interplanar distance for the (hkl) crystallographic direction (which is $d/\sqrt{2}$), n_{eff} the effective refractive index of the material, and θ the angle between the incident radiation and the normal to the set of crystalline planes determined by the (hkl) indices. The effective refractive index n_{eff} can be calculated by the following equation[19]:

$$n_{\mathrm{eff}} = (\phi_1 n_{\mathrm{PMMA}}^2 + \phi_2 n_{\mathrm{Air}}^2)^{1/2} \tag{2}$$

where ϕ_1 and ϕ_2 are the volume fractions of the PMMA and air voids, which are 0.74 and 0.26, respectively, for a close-packed fcc structure. n_{PMMA} and n_{Air} are the refractive indices of PMMA and air, which are 1.49 and 1, respectively. Substituting d_{111}, n_{eff}, and $\theta = 0^{\mathrm{o}}$ into Eq. (1), we obtain that the reflection from the (111) planes under the angle of normal incidence should produce a maximum at λ =546 nm, which is very close to the transmittance spectrum shown in Fig. 3.

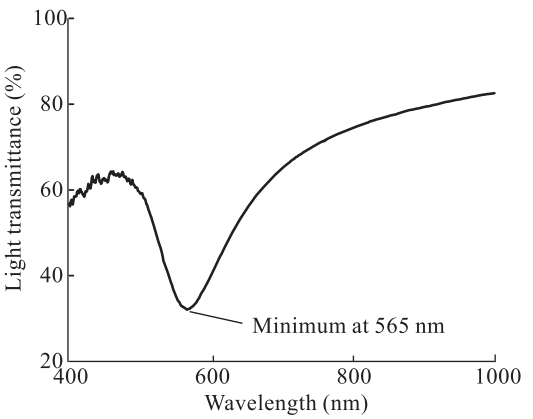

Fig. 3 Light transmittance through ordered PMMA array with fcc structure on Anopore support

The TGA-DSC analysis was carried out with PMMA spheres in order to understand the thermal stability and identify the glass transition temperature of these PMMA arrays. Figure 4 shows the weight loss

and heat flow of PMMA spheres as a function of temperature. There is very little weight loss below 260℃, and a 100% weight change from 260-380℃ occurs due to the decomposition of PMMA spheres. In the heat flow curve, the endothermic peak at 130℃ represents the transition of PMMA spheres from a glassy to rubber state (the glass transition temperature). The peak at 175℃ corresponds to the melting of the spheres, and the strong peaks above 250-300℃ correspond to the decomposition of the PMMA spheres.

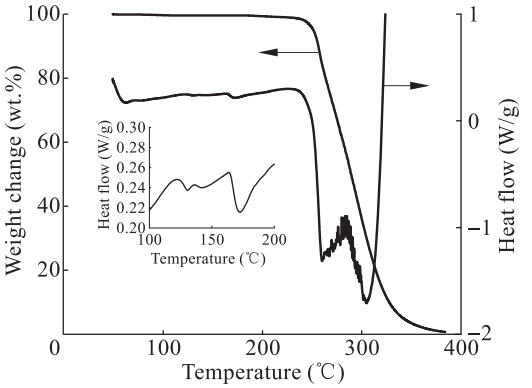

Fig. 4 TGA-DSC of PMMA spheres

When the 3-D PMMA arrays on the Anopore support were used without further treatment as the template for the infiltration of silica matrix to obtain the final reverse opal membrane on the Anopore support, the silica layer cracked and peeled off from the Anopore substrate upon drying, due to the stress induced by the drying process and weak stress tolerance of the 3-D PMMA arrays. Annealing the PMMA template arrays at its glass transition temperature for 1 h was found to be effective to improve the mechanical strength and enhance the adhesion between the silica layer and alumina support, because at the glass transition temperature of PMMA spheres their branches (or segments) became soft and may move relative to one another and cross each other, having PMMA spheres annealed together enhancing the mechanical strength of the template layer.

2.2 Ordered macroporous silica pellets and membrane

Unsupported macroporous silica pellets of 5-10 mm in sizes were prepared by using the pellets of ordered PMMA arrays as the template, prepared by centrifugation without subsequent annealing treatment. The 3-D ordered macroporous silica pellets were obtained by infiltrating silica sol into the 3-D PMMA arrays, followed by drying and calcination to remove the template. The structure of ordered macroporous silica is shown in Fig. 5. The silica has a reverse opal structure determined by the structure of 3-D PMMA array. The diameter of the spherical pores is 200 nm, which is smaller than the diameter of the PMMA spheres used as the template (240 nm) due to the shrinkage of the silica network during calcination. The three black circles under each pore are the windows through which the pore is connected to the other three pores underneath. The diameter of the windows is about 1/7 of the sphere size.

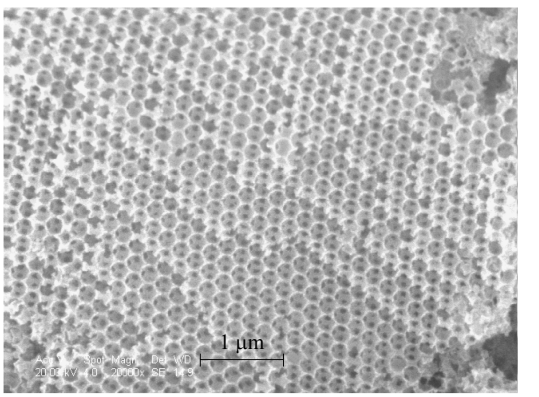

Fig. 5 SEM image of macroporous silica material. The PMMA template was removed by calcination.

Nitrogen adsorption/desorption isotherms of this silica material are shown in Fig. 6. Figures 6a and 6b show the N_2 adsorption isotherm of the silica after the template was removed by solvent extraction and calcination, respectively. According to the Brunauer, Deming, Deming, and Teller (BDDT) classification[20], these two isotherms correspond to a combination of Type I and Type IV isotherms with H3 hysteresis[21]. The initial steep portion of the curve is due to the contribution of the micropores. The obvious hysteresis loop is typical of mesoporous and macroporous materials displaying interconnected pores of wide range of sizes and shapes[22].

The same silica sol used to prepare the reversed opal structured silica was also poured into a Petri dish without the PMMA sphere template and dried in air, followed by calcination at 550℃ in air for 3 h. Figure 7 shows the nitrogen adsorption isotherm of the sol-gel derived silica. This adsorption isotherm was found to be Type I, which confirms the microporous structure of the sample. The Horvath-Kawazoe differential pore

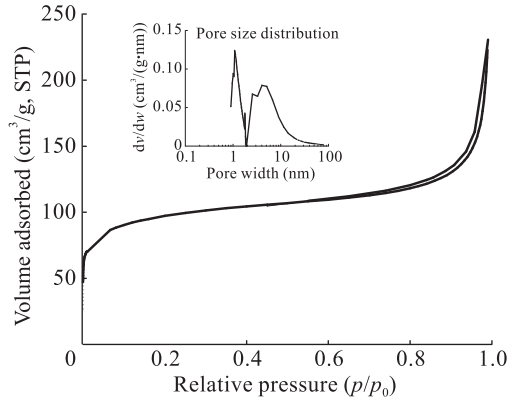

(a) Template removed by solvent extraction

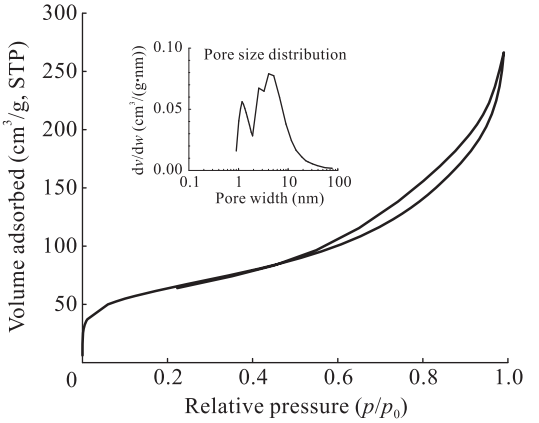

(b) Template removed by calcination

Fig. 6 N_2 adsorption/desorption isotherms and pore size distributions of ordered macroporous silica prepared using 3-D PMMA array as the template

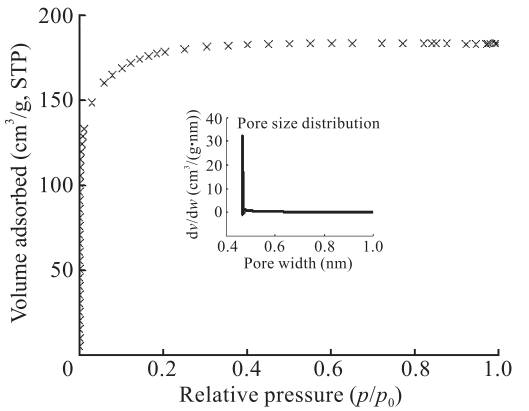

Fig. 7 Adsorption/desorption isotherms and pore size distribution of sol-gel derived silica prepared without template

volume plot shows that the materials have pores with diameters about 0.5 nm. It is well known that the acid catalyzed sol-gel process proceeds through hydrolysis and condensation resulting in polymeric silica sol. The silica film derived from the polymeric sol has a micropore structure with pore size smaller than 1 nm[18].

Table 1 shows the average micro- and meso-pore size of sol-gel derived silica and ordered macroporous silica with template removed by calcination and solvent extraction methods. The silica prepared without the template has 0.6 nm micropores showing a very narrow pore size distribution and the absence of pores in the mesoporous range. However, the silica material prepared using PMMA as the template has both micropores and mesopores. The micropores of the silica prepared using the PMMA template are larger than those for the silica prepared without the PMMA spheres. Such a difference in micropore size is caused by the difference in the drying rate. The drying rate of the silica prepared using the PMMA template is slower than in the case of silica prepared without the template due to the limited mass transfer rate of solvent inside the template layer. The mesopores correspond to the windows connecting the spherical macropores. As compared with solvent extraction method for template removal, calcination method gives smaller micropores due to the shrinkage of the frame work of the silica material, and larger average mesopores because calcinations induced more cracks than solvent extraction, which has wilder conditions. The macropores can not be detected by the nitrogen adsorption method and are instead observed visually by SEM.

Table 1 Pore size of silica samples prepared using PMMA as the template (template were removed by calcination or solvent extraction) and microporous silica prepared without the template

Template removal method	Horvath-Kawazoe median pore width (nm)	BJH average pore diameter (nm)
Template free	0.6	–
Calcination	1.0	12
Solvent extraction	1.2	8

Ordered macroporous silica membranes were prepared on Anopore supports using PMMA arrays deposited by the filtration method and subsequent removal of the template by calcination. Calcination was applied because it showed better removal of template than solvent extraction method. Figures 8a and 8b show the top surface and cross-section of the macroporous silica membrane. This macroporous silica membrane displays interconnected 3-D spherical pores. Each spherical pore represents a negative replica of one PMMA sphere. The macroporous silica membrane is about 8 μm in thickness. The pore structure of the macroporous silica

membrane is not as ordered as that in the free standing macroporous silica (Fig. 5) because the template prepared on Anopore alumina support is not as ordered as the template prepared by centrifugation due to the influence of the pore morphology of the support.

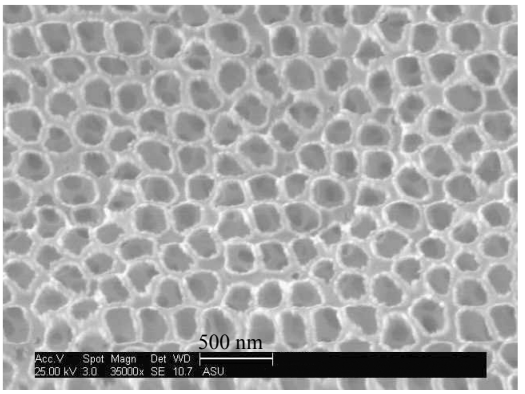

(a) Top view

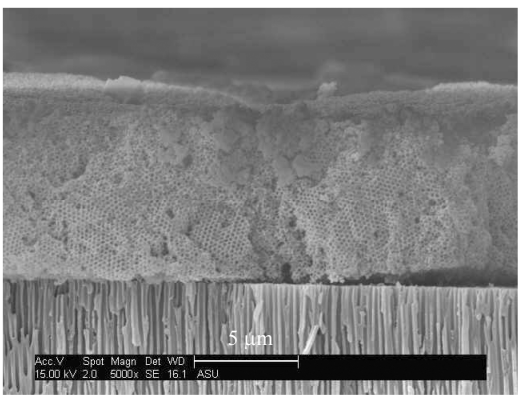

(b) Cross-section

Fig. 8 SEM photographs of a macroporous silica membrane

3 Conclusions

We have described an effective method to prepare ordered 3-D macroporous silica membrane on porous Anopore alumina support. This method is based on the template-directed sol-gel process, in which monodisperse colloidal PMMA spheres were self-assembled into ordered 3-D PMMA arrays on the support by vacuum filtration using the support as a filter. The 3-D PMMA arrays were annealed at its glass transition temperature for 1 h to improve the mechanical strength of the template layer and enhance the adhesion between the silica membrane and the alumina substrate. Multiple infiltrations of silica sol-gel were used to fill the gaps generated during the drying process due to the shrinkage of the silica network. The membranes prepared by this method have well-defined, uniform pores, and are highly promising for applications in chemical separation, photonic technology, drug delivery, as well as membrane reactors.

Acknowledgements

The authors gratefully acknowledge the center for Solid State Science at Arizona State University for the use of their facilities.

References

[1] Tanev P T, Chibwe M, Pinnavaia T J. Titanium-containing mesoporous molecular sieves for catalytic oxidation of aromatic compounds. *Nature*, 1994, **368**: 321-323.

[2] Schilling J, Scherer A, GÖsele U, et al. Macroporous silicon membranes as electron and X-ray transmissive windows. *Applied Physics Letters*, 2004, **85**(7): 1152-1154.

[3] Siegel R A, Langer R. Mechanistic studies of macromolecular drug release from macroporous polymers, II: Models for the slow kinetics of drug release. *Journal of Controlled Release*, 1990, **14**(2): 153-167.

[4] Angelucci R, Poggi A, Dori L, et al. Permeated porous silicon suspended membrane as sub-ppm benzene sensor for air quality monitoring. *Journal of Porous Materials*, 2000, **7**(1-3): 197-200.

[5] Cichelli Julie, Zharov Ilya. Chiral permselectivity in surface-modified nanoporous opal films. *Journal of American Chemical Society*, 2006, **128**: 8130-8131.

[6] Zeng Y, Harrison D J. Self-assembled colloidal arrays as three-dimensional nanofluidic sieves for separation of biomolecules on microchips. *Anal. Chem*., 2007, **79**: 2289-2295.

[7] Zheng S, Ross E, Legg M A, et al. High-speed electroseparations inside silica colloidal crystals. *Journal of American Chemical Society*, 2006, **128**(28): 9016-9017.

[8] Guliants V V, Carreon M A, Lin Y S. Ordered mesoporous and macroporous inorganic films and membranes. *Journal of Membrane Science*, 2004, **235**(1-2): 53-72.

[9] Arora A K, Tata B V R. Ordering and phase transitions in colloidal systems. VCH, Weinheim, 1996.

[10] Gast A P, Russel W B. Simple ordering in complex fluids. *Physics Today*, 1998, **51**(12): 24-29.

[11] Park S H, Qin D, Xia Y. Crystallization of mesoscale particles over large areas. *Advanced Material*, 1998, **10**(13): 1028-1032.

[12] Holland B T, Blanford C F, Stein A. Synthesis of macroporous minerals with highly ordered three-dimensional arrays of spheroidal voids. *Science*, 1998, **281**(5376):

538-540.

[13] Turner M E, Trentler T J, Colvin V L. Thin films of macroporous metal oxides. *Advanced Material*, 2001, **13**(3): 180-183.

[14] Ye Y H, Badilescu S, Truong V V. Large-scale ordered macroporous SiO_2 thin films by a template-directed method. *Applied Physics Letters*, 2002, **81**(4): 616-618.

[15] Uhlhorn R J R, Keizer K, Burggraaf A J. Gas transport and separation with ceramic membranes, Part II: Synthesis and separation properties of microporous membranes. *Journal of Membrane Science*, 1992, **66**(2-3): 271-287.

[16] Lovell A Peter, El-Aasser Mohamed S. Emulsion Polymerization and Emulsion Polymers. New York: J. Wiley, 1997.

[17] Woodcock L V. Reply: Entropy difference between crystal phases. *Nature*, 1997, **388**: 236.

[18] Astratov V N, Adawi A M, Fricker S, et al. Interplay of order and disorder in the optical properties of opal photonic crystals. *Physical Review B*, 2002, **66**(16): 165 215-165 217.

[19] Le T V, Ross E E, Velarde T R C, et al. Sintered silica colloidal crystals with fully hydroxylated surfaces. *Langmuir*, 2007, **23**(16): 8554-8559.

[20] Sing K S W, Everett D H, Haul R A W, et al. Reporting physisorption data for gas/solid systems, with special reference to the determination of surface area and porosity. *Pure Applied Chemestry*, 1985, **57**(4): 603-619.

[21] Gregg S J, Sing K S W. Adsorption, Surface Area and Porosity. 2nd edition. London: Academic Press, 1982.

[22] Webb P A, Orr C. Analytical Methods in Fine Particle Technology. Micromeritics Instrument Corporation, Norcross, GA, USA, 1997.